How Solvents Affect Acetaminophen Etching Pattern Formation: Interaction between Solvent and Acetaminophen at the Solid/Liquid Interface

Hong Wen, Tonglei Li, Kenneth R. Morris,* and Kinam Park

Department of Industrial and Physical Pharmacy, Purdue University, West Lafayette, Indiana 47907-1336

The objective of this work was to further elucidate the dissolution process of acetaminophen crystals at the molecular level. The differences in the etching patterns from different solvents were used to study the interactions between solvent and acetaminophen molecules at the solid−liquid interface, such as solubilizing ability and potential solvent adsorption. The predicted etching patterns, based on the projections of attachment energies on the corresponding faces together with the solubilizing ability of the solvents, fit the observed etching patterns well. On the (001) face, the etching patterns were predominantly in the direction of the *a*-axis, which was also the direction of the dominant attachment energy. On the (110) face, the etching patterns were consistently in the direction of the *c*-axis irrespective of solvent used, and they were variable in other directions. These were well fit by the predicted etching patterns accounting for the different solubilizing ability of solvents. Both the most significant etching pattern deviations (on the (010) face) and the most significant morphology changes were observed with dichloroethane for acetaminophen. The morphology of acetaminophen crystals from different solvents showed that only the crystals from dichloroethane had significant elongation along the *c*-axis, which suggests the existence of stronger adsorption in the *a*-axis and *b*-axis directions than along the *c*-axis for dichloroethane. Overall, the current work suggests that the crystal interaction network, together with the interactions between solvent and acetaminophen, affects surface diffusion and plays an important role in the dissolution process.

Introduction

It is well-known that the dissolution processes of drug crystals may affect bioavailability, and developing a better understanding of the dissolution processes may help to optimize the desired therapeutic effects. Crystal habit is often an important factor in influencing intrinsic dissolution rate.[1−3] Crystal habits can also affect many physical properties, such as ability to flow, compressibility, crystal face wettability, and dissolution rate anisotropy.[4] For aspirin crystals, the dissolution rate of the (100) face was observed to be approximately 6 times faster than that of the (001) face [3]. Generally, the different dissolution rates of different faces are attributed to the anisotropy of the crystal structure.[5] However, anisotropy alone cannot explain why the dissolution rate is higher on a certain face. The attachment energies on different faces are often significantly different and therefore may contribute to the dissolution rate differences between faces. The reciprocal nature of the forces at work in dissolution and crystallization also make this topic important in the molecular level elucidation of crystal growth.

Etching patterns have been quite widely studied to help understand crystal structures, as well as the effects of crystal structures and solvents on dissolution.[6−10] The positions of the etching patterns are generally agreed to be related to the sites of defects on the crystal surface, and the observation of the etching pits can be used as a tool for studying crystal dislocations in the dissolution. Li et al.[7] also reported that surface diffusion

plays a very important role in the generation of etching pattern shape. By affecting surface diffusion, the crystal structure can influence the shape of etching pits based on the directionality of the attachment energies. The etching patterns formed by different solvents are often dissimilar, and therefore, the effect of solvents cannot be ignored. It is assumed that solvent molecules can adsorb onto a crystal surface, interrupt the original interaction network within the crystal structure, and cause new etching patterns depending upon the structure of the solvents.[7] Therefore, the etching pattern can be influenced not only by the crystal structure but also by the interactions between molecules in the lattice and solvent molecules. Only limited reports have been published on the effect of solvents on crystal dissolution at the molecular level, and more study is needed to better understand the interactions between solvent and crystal.

The dissolution process may not only be beneficial in improving understanding of the interactions between molecules at crystal surfaces and solvents during the dissolution process but may also lend understanding to solvent-induced polymorphic transformation.[11] Because of the weak and dynamic interactions between solvent and molecules at crystal surfaces, traditional approaches (e.g., osmotic pressure, UV) may not be sensitive enough to detect interactions at the solid−liquid interface. On the basis of the difference in etching patterns in different solvents, these interactions may be deduced.

In *periodic bond chain (PBC) theory*, Hartman & Perdok proposed the concept of "attachment energy", that is, the bond energy released when one building unit is attached to the surface of a crystal face.[12−14] This theory has been successfully used in crystal morphology prediction.[15,16] In this formalism, any solvent present during the crystallization process may be treated

* To whom correspondence should be addressed. Kenneth R. Morris, Ph.D., Professor and Associate Head, Department of Industrial and Physical Pharmacy, Purdue University, 575 Stadium Mall Drive, Room 112, West Lafayette, IN, 47907. Tel: (765) 496-3387. Fax: (765) 494−6545. E-mail: morris@pharmacy.purdue.edu.

as an "additive".[17] The crystal face that has stronger interactions with the solvent will grow more slowly than the face that has weaker interactions. The crystal morphology change in different solvents is an indication of the interactions between solvent and crystal. The deviation of the crystal morphology from the predicted morphology can provide specific information about the interactions between the crystal molecules and the solvent molecules and, hence, the dissolution process.

In the current research, attachment energies were calculated using Cerius[2] software on the basis of the crystal structures acquired from the Cambridge structural database [18] and appropriately selected force fields. A key extension of the earlier hypothesis is the assumption that even if two molecules are not on the same face, the contribution of the attachment energy between a subsurface molecule and a surface molecule may play a role. By linear transformation (projection) of those PBC vectors of the attachment energies on the faces of interest, all of the attachment energies related to the face of interest can be incorporated. It is assumed that there may be elongation in the etching patterns in the direction of stronger attachment energy relative to the direction(s) with weaker attachment energy. Solvents may also affect etching pattern formation through their surface diffusion time. A model has been proposed to combine the contributions of attachment energy and solvent on predicting etching pattern formation and to help better understand the dissolution process.

While historically optical microscopy was the primary tool for the study of crystal growth, atomic force microscopy (AFM) represents a new generation of nanoscale surface characterization methods. AFM has been widely used for the observation of protein crystal growth or dissolution at the molecular level.[19−25] The high-resolution three-dimensional surface images scanned by the AFM can provide more information about dissolution than the two-dimensional images obtained from optical microscopy.

Experimental Section

Single-Crystal Preparation. The single crystals of acetaminophen were prepared from acetaminophen raw materials (USP, Amend Drug & Chemical Co., Irvington, NJ) by seeding in supersaturated solution. The average size of the single crystals was between 1 and 2 mm.

Face Indexing by X-ray Measurement. The indices of single crystals were measured by a powder X-ray diffractometer (XRD-6000, Shimadzu, Kyoto, Japan). Each measured crystal was mounted onto one AFM sample disk, and the measured face was adjusted to be parallel to the disk surface. The AFM disk was placed on the X-ray diffraction sample holder. Generally, the scan range was from 10° to 40° with a step size of 0.02°. The X-ray source was Cu K radiation, and the voltage and current were set at 40.0 kV and 40.0 mA, respectively. For those small faces, the crystal was rotated at 60 rpm to acquire the specific face diffraction information.

Axis Identification. The theoretical two-dimensional crystal morphology on each face, as well as the directions of axes, was derived from the simulation of three-dimensional crystal structure. The axis directions of interest on single crystals were determined by comparing the observed crystal face with the theoretical crystal morphology and direction map.

Partial Dissolution. The six solvents used for dissolution tests were deionized distilled water, acetone (EM Science, Gibbstown, NJ), ethyl acetate (Mallinckrodt Baker, Paris, KY), acetic anhydride (Aldrich Chemical, Milwaukee, WI), (1,2)-dichloroethane (Aldrich Chemical, Milwaukee, WI), pyridine

TABLE 1: Etching Agents and Etching Duration for (001), (110), and (010) Faces

etching agent	etching duration (sec)		
	$(001)^a$	(110)	(010)
H_2O	120	120	60
CH_3COCH_3/CCl_4 (1:1 v/v)	20	10	15
$(CH_3CO)_2O/CCl_4$ (1:1 v/v)	30	15	15
$CH_3COOC_2H_5/CCl_4$ (1:1 v/v)	30	15, 30	15
$ClCH_2CH_2Cl$	60	30, 60	60
C_5NH_5/CCl_4 (1:5 v/v)	10	10	15

^{a} For (001) face, acetone, acetic anhydride, and ethyl acetate were pure solvents.

TABLE 2: Acetaminophen Crystallization in Different Solvents

| solvent	condition	S^a
water	4.53 g/250 mL	0.25
dichloroethane	0.115 g/400 mL	0.44
acetic anhydride	2.25 g/200 mL	0.25
acetone	4.20 g/50 mL	0
ethyl acetate	2.00 g/200 mL	0.25
pyridine	4.70 g/10 mL	0

^{a} S = concentration/solubility − 1.

(Aldrich Chemical, Milwaukee, WI), and carbon tetrachloride (Aldrich Chemical, Milwaukee, WI). The dissolution tests were performed at room temperature, and the time varied from 10 to 120 s. After a predetermined time, the disk was taken from the solution, and the remaining solution on the crystal surface was removed with filter paper. Compressed air was used to further remove residual solution from the crystal surface. Finally, the sample was air-dried at least 1 h before AFM observation. Experimental conditions for partial dissolution are listed in Table 1.

Crystallization in Different Solvents. Acetaminophen was crystallized from the six solvents used in partial dissolution tests. All supersaturated solutions were filtered with a 0.2 μm filter and left at room temperature to dry slowly. Experimental conditions for crystallization in different solvents are listed in Table 2. The supersaturation ratio in water was based on the measured acetaminophen solubility of 14.5 mg/mL at 25.0 °C. The supersaturation ratios (S) for other solvents were calculated on the basis of the published acetaminophen solubility.[7]

AFM Measurement. The surfaces of single acetaminophen crystals were observed with an AFM (NanoScope Multi-Mode AFM, Digital Instruments, Inc., Santa Barbara, CA). AFM observations were carried out in contact mode at room temperature using a J-type piezo-scanner, and the tips were standard silicon nitride probes. For each observation, images in both the deflection mode and the height mode were saved. The images in the following sections were in the deflection mode unless otherwise specified.

PBC Calculation. The PBC vectors of an acetaminophen crystal were calculated with Cerius[2] 4.2 (Molecular Simulation, Inc., San Diego, CA) based on the crystal structure of acetaminophen from the Cambridge Structural Database (HXACAN01) [18] with the following parameters: $P_{2/1a}$; $a = 12.93$ Å, $b = 9.4$ Å; $c = 7.10$ Å; $\beta = 115.9°$. After the current energy for the acetaminophen crystal was calculated, the PBC vectors were calculated using the following settings: the force field was Dreiding 2.21; the partial atomic charges were calculated using the equilibrium method, Gasteiger-Quanta 1.0; the van der Waals interaction and Coulomb forces were set with the Ewald summation.

How Solvents Affect Acetaminophen Etching Pattern
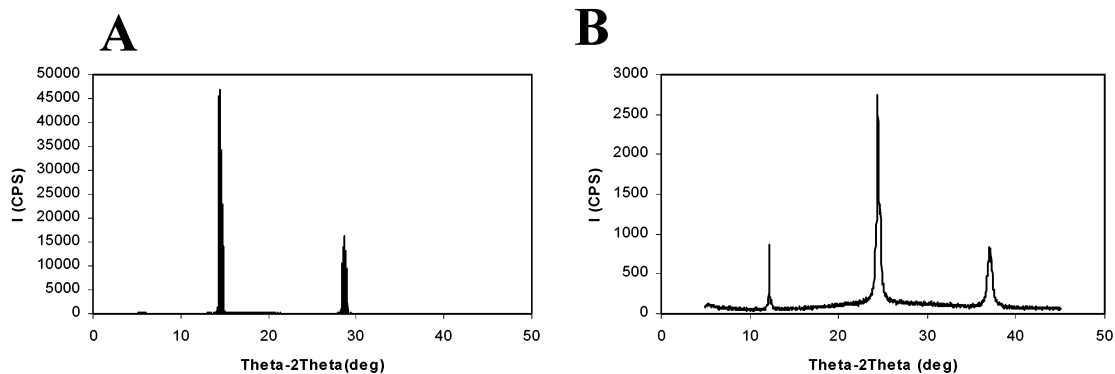
Figure 1. X-ray diffraction patterns of the acetaminophen faces: (A) the pattern for the (001) face with 2θ values of 14.3149° and 28.7030° (28.6086°); (B) the pattern for the (110) face with 2θ values of 12.1590°, 24.4045°, and 36.9400°.

TABLE 3: X-ray Diffraction Information for Acetaminophen

h	k	L	d-spacing	2θ	I	I%
1	1	0	7.3110	12.105	127 042	27.14
2	2	0	3.6555	24.349	386 710	82.62
3	3	0	2.4370	36.882	64 110.6	13.70
0	0	1	6.3869	13.865	186 705	39.89
0	0	2	3.1934	27.938	24 691.7	5.28
0	2	0	4.7000	18.881	12 216.7	2.61

[a] I is the integrated intensity. [b] $I\%$ = the peak intensity/the highest peak intensity.

Results and Discussion

The basic approach employed was to observe the etching patterns on the (001) and (110) faces of acetaminophen. A model in which the PBCs were projected onto the faces of interest was proposed to study the effects of attachment energies on etching pattern formation. By comparing the predicted etching patterns with the observed etching patterns, we explained the interactions between solvent and drug molecules at the interface. To study whether solvent adsorption also occurs during the crystallization process, the morphology of acetaminophen crystals from different solvents have been investigated.

Indexing the Faces of Acetaminophen Single Crystals. Single crystals of acetaminophen for the etching experiment were grown in water. The (110) face (largest and 4-fold degenerate), as well as the (001), (011), and (20$\bar{1}$) were the growth faces of the single crystals. The (010) face is internal and may be exposed by cleaving single crystals. Before executing the etching experiment, we indexed the tested face by X-ray diffraction, and its axis direction was determined as described.

The simulated X-ray powder diffraction patterns for Cu Kα were calculated using Cerius[2] 4.2 (Table 3). Figure 1 shows the X-ray diffraction of (001) and (110) faces for acetaminophen. The area of the (001) faces were small and required rotating the crystal during the powder diffraction experiment. Because the crystal surfaces were often not at the same level as the sample holder, the peaks from crystals of different sizes were slightly shifted resulting in some "splitting". This notwithstanding, the faces were indexed by this method.

AFM Observation of Etching Patterns on the (001) Face. On the (001) face of the acetaminophen crystals, there are two perpendicular crystallographic axes: the a-axis and the b-axis. Each acetaminophen molecule forms four hydrogen bonds with other acetaminophen molecules, two of which are NH···OH linking acetaminophen molecules along the a-axis.

All of the etching patterns on the (001) face included a feature along the a-axis, which is the hydrogen-bonding chain direction, as well as the direction of the dominant PBC. Figures 2 and 3
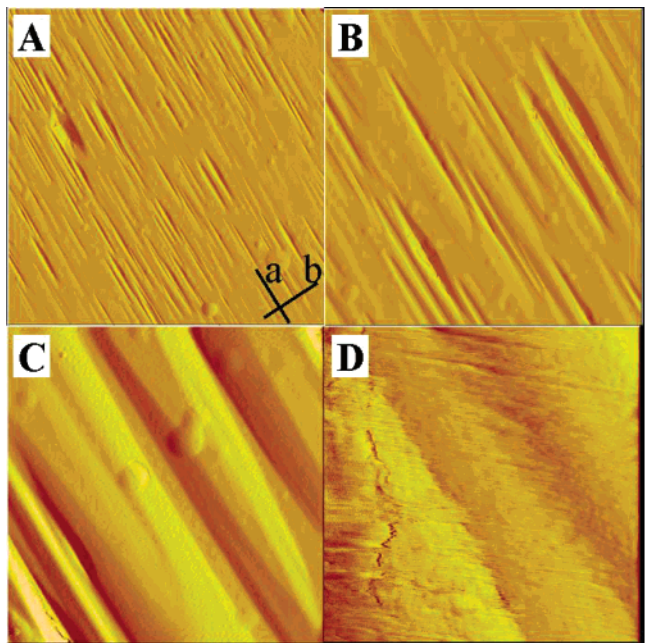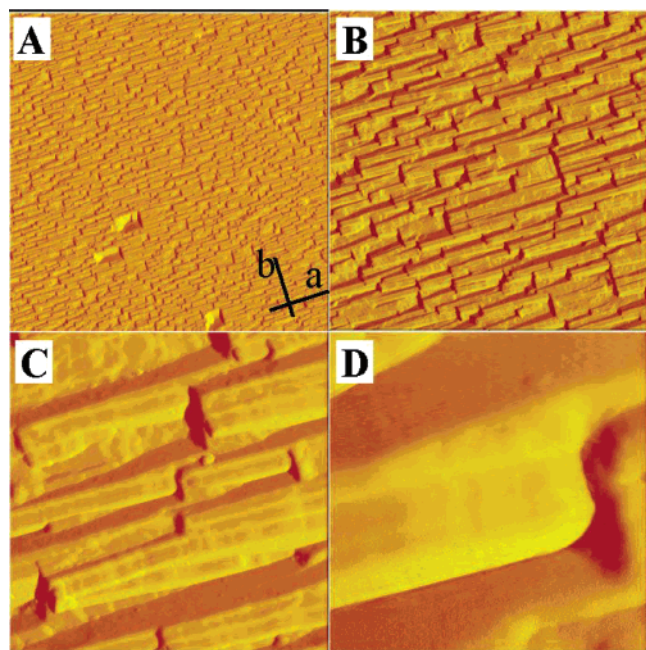

Figure 2. AFM images of the (001) face of an acetaminophen crystal dissolved in pyridine/CCl$_4$ (1:1 v/v) for 30 s. The image sizes are (A) 60×60, (B) 20×20, (C) 5×5, and (D) 1×1 μm^2. From panels A to D, the images were zoomed in gradually. The a- and b-axes are shown in panel A.

show the etching patterns of the (001) face of acetaminophen crystals created by pyridine/CCl$_4$ (1:1 v/v) and by dichloroethane, respectively. The etching patterns created by water, acetic anhydride, ethyl acetate, and pyridine are all narrow slits of continuous depth along the a-axis.

The etching pattern created by dichloroethane resembles an elongated "bar" along the a-axis, with the end of the bar paralleling the b-axis (approximately perpendicular to the (001) face). Figure 4 shows the height profile of the etching pattern created by dichloroethane. The bar is narrow and deep along the a-axis direction, and at the end of the bar, the height changes abruptly. This is consistent with dichloroethane strongly adsorbing onto the crystal surface along the a-axis and disrupting surface diffusion to some degree. Thus, even though the attachment energy along the a-axis is dominant on the (001) face, the strong adsorption by dichloroethane caused etching patterns to change from their normal slit shape to the foreshortened bar shape. Li et al.[7] reported that on the (010) face of acetaminophen, the simulated etching pattern by dichloroethane should be significant in both the a- and c-directions and particularly that it should be dominant in the direction of the a-axis. The actual observed etching pattern by dichloroethane,

Figure 3. AFM images of the (001) face of an acetaminophen crystal dissolved in 1,2-dichloroethane for 2 min. The image sizes are (A) 60 × 60, (B) 20 × 20, (C) 5 × 5, and (D) 1 × 1 μm^2, respectively. From panels A to D, the images were zoomed in gradually. The a and b axes are shown in panel A.
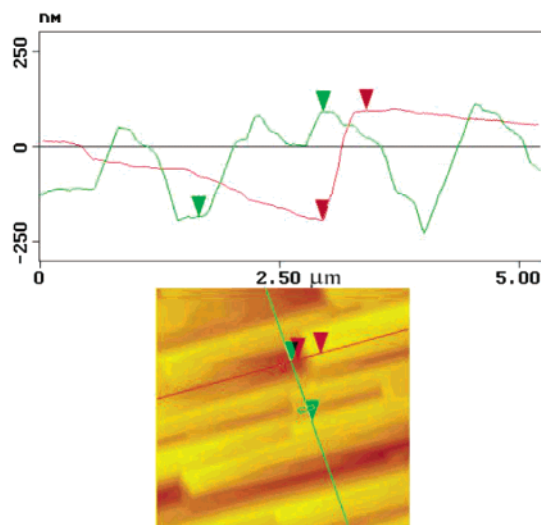
Figure 4. Height profile taken along lines on height image, corresponding to Figure 3c of the (001) face by dichloroethane.

however, is a long, narrow slit along the c-axis on the (010) face. The phenomenon is consistent with and may be explained by the observation on the (001) face.

The etching pattern of the (001) face created by acetone is also slit like; however, it is much wider than the slits produced by the other solvents. Its height profile does not show any abrupt change in the slit direction; that is, the a-axis direction. Because of the relatively small size of acetone and its hydrogen-bond-accepting capability, acetone may form hydrogen bonds with both hydrogen-bond chains. One hydrogen-bond chain is in the direction of a-axis, and the other is in the direction intermediate between the a- and c-axes. The acetaminophen crystallized from acetone exhibits more faces than that from water, which may imply stronger adsorption of acetone in many directions (certainly on those fast growing faces in water). Both the adsorption of acetone onto the crystal surfaces and the high solubility may contribute to the width of the observed etching patterns.

**AFM Observation of Etching Patterns on The (110) Face.** The four largest faces of the acetaminophen single crystals grown in water are the (110) family of faces; thus, the dissolution process for the (110) face may affect the overall dissolution rate. Figures 5, 6, and 7 show the etching patterns of the (110) face created by acetic anhydride and ethyl acetate, acetone and pyridine, and dichloroethane and water, respectively. All of the etching patterns share a feature along the c-axis. However, the etching patterns are solvent-dependent in the other directions. The etching patterns of the (110) face by acetic anhydride, acetone, and pyridine are arclike, their diameter is along the c-axis, and it is difficult to evaluate any dependence of the arc on the projection direction along the a-axis or b-axis on the (110) face. However, closer examination shows a possible "blurring" of edges formed along the a ($-a$) cutting the edge formed in the c direction. The directionality of the etching pattern formed by water is not very clear, even though it does have a certain preference in the c direction; it may be that water causes "kinetic roughening" of the face.[26] For ethyl acetate, the etching pattern is angular with one side along the c-axis. The etching pattern created by dichloroethane looks like an arrowhead with one side along the c-axis and the base along the b-axis and is narrower than the other patterns. Overall, the etching patterns on the (110) face are much more complex relative to those on the (001) face, and it is interesting to compare these etching patterns with the directionality and strength of the PBC vectors related to the (110) face.

Acetaminophen molecules are connected by hydrogen bonds along the a-axis as well as in a direction intermediate between the a-axis and the c-axis on the (010) face but not in the direction of the c-axis (though a strong van der Waals interaction does exist in the c direction). On the (010) face, the etching patterns created by all of the solvents are consistently in the direction of the c-axis, but they are highly solvent-dependent in the direction of the a-axis.[7,8] On the (110) face, the etching patterns by different solvents are also consistently in the direction of the c-axis, but they are variable in the direction of the *projection* of the a-axis on the (110) face. Solvent molecules may attach to a crystal surface along the a-axis by hydrogen-bonding interactions, thus affecting further dissolution along the a-axis. Solvents cannot form a hydrogen bond with acetaminophen in the direction of c-axis, which may contribute to the stable etching feature in the direction of the c-axis by various solvents. It is worthwhile to compare the observed etching patterns with the predicted etching patterns to study whether the etching patterns are dominated by such projections together with the solubilizing ability of solvents or are affected by solvent adsorption.

Surface Adsorption of Solvents on Crystal Morphology. The effects of solvent on crystal morphology have been widely reported, and the specific adsorption of solvent on different faces may play a very important role in crystal morphology.[27,28] If solvents have a specific adsorption during the dissolution process, a corresponding adsorption in the crystallization process of acetaminophen may be observed. Among the acetaminophen crystals grown in six different solvents, only the crystals in dichloroethane are needlelike, and crystals in the other five solvents are approximately parallelepiped.

X-ray diffraction experiments also confirm that the dominant faces of needlelike crystals grown in dichloroethane are the (110) family. The published reports,[29,30] as well as our observations, show that the initial supersaturation ratio does not affect the crystal habit in aqueous solutions if the supersaturation is greater than approximately 15%. For the crystals grown from the
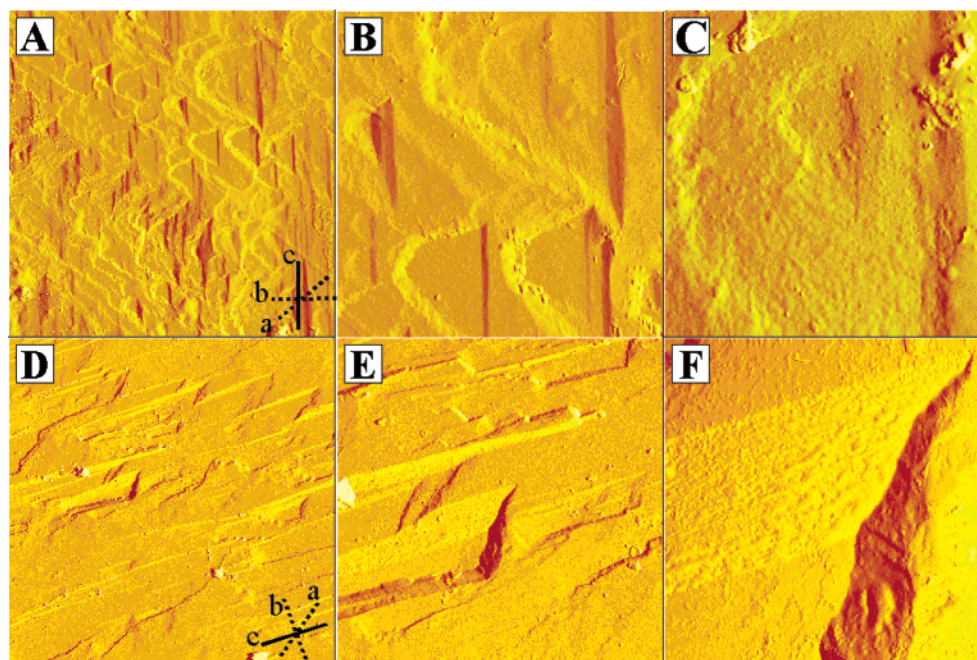
Figure 5. AFM images of the (110) face of an acetaminophen crystal dissolved in acetic anhydride (A,B,C) and ethyl acetate (D,E,F). The image sizes are (A,D) 6060 μm^2, (B,E) 2020 μm^2, and (C,F) 55 μm^2. From panels A to C, as well as panel D to F, the images are zoomed in gradually. The *c*-axis, as well as the projections of the *a*- and *b*-axes, on the (110) face are marked in panels A and D.
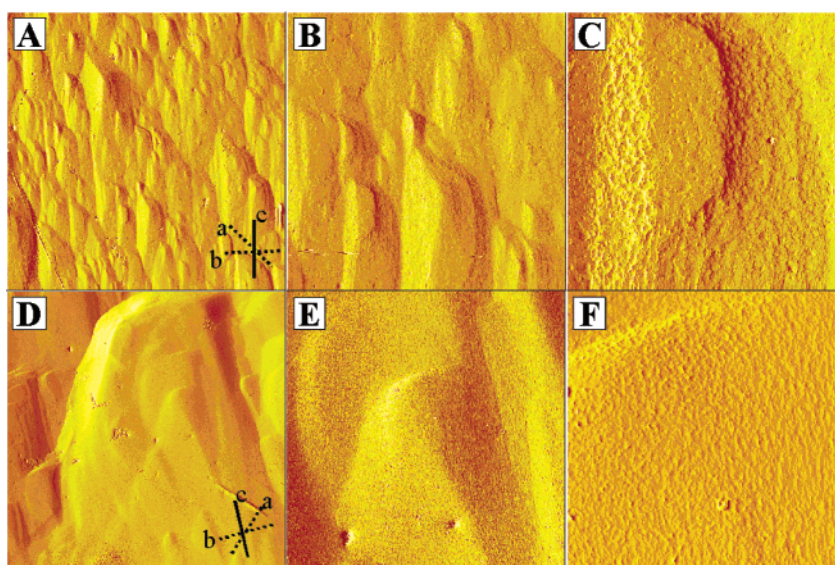
Figure 6. AFM images of the (110) face of an acetaminophen crystal dissolved in acetone (A, B and C) and pyridine (D, E and F). The image sizes are (A,D) 6060 μm^2, (B,E) 2020 μm^2, and (C,F) 55 μm^2. From (A) to (C), as well as (D) to (F), the images are zoomed in gradually. The *c*-axis, as well as the projections of the *a*-axis and *b*-axis on the (110) face, are marked on A and D.

dichloroethane solution, with supersaturation as high as 44%, it is very likely that the significant morphology deviation from ideal morphology, predicted by Cerius^2 4.2 on the basis of BFDH simulation, was attributable to the specific adsorption of dichloroethane onto acetaminophen crystals. The most significant deviation of etching patterns was observed from etched by dichloroethane on the (010) face.[7] On the (010) face, the etching patterns created by dichloroethane are slits along the *c*-axis and have no obvious elongation along the *a*-axis such as that observed using other solvents. The deviations in both crystal morphology and etching patterns suggest that the adsorption for dichloroethane along the *c*-axis should be much weaker than that along the *a*- and *b*-axes.

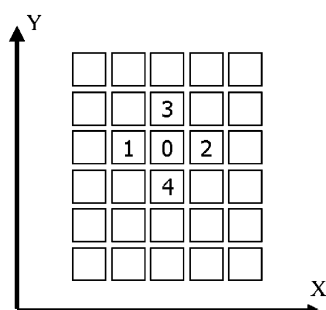**Effects of Attachment Energies on Surface Diffusion.** Li et al. reported that surface diffusion is under the guidance of the supramolecular interaction network,[7] that is, that different attachment energies in different directions cause etching patterns to have directional preference. In addition to solvent adsorption on the crystal surface, the solubilizing ability of the solvent will affect surface diffusion time constants. Even though there are many factors that can affect surface diffusion, it is still useful to expand the use of the model to elucidate the effects of attachment energies on surface diffusion and etching patterns.

In the dissolution process, detachment of molecules from the lattice is affected by the attachment energy in different directions. The initial assumption is that there are no molecules at the 0 lattice site and that sites 1, 2, 3, and 4 have been occupied by molecules in the lattice in Figure 8. To detach one of the four molecules from the lattice, the attachment energies between the molecule and its neighboring molecules around and below
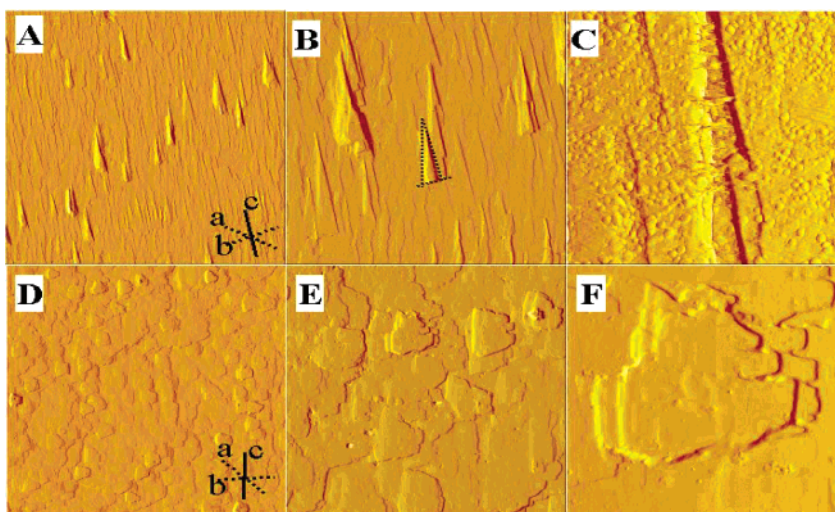
Figure 7. AFM images of the (110) face of acetaminophen crystals dissolved in dichloroethane (A,B,C) and water (D,E,F). The image sizes are (A,D) 6060 μm², (B,E) 2020 μm², and (C,F) 55 μm². From panels A to C, as well as panels D to F, the images are zoomed in gradually. The *c*-axis, as well as the projections of the *a*- and *b*-axes on the (110) face, are marked in panels A and D.

Figure 8. The relationship between the directions of attachment energies and the directions of adsorption and desorption of surface diffusing molecules, assuming that the attachment energy in the *Y* direction is stronger than that in the *X* direction.

it need to be overcome. Assuming that the interaction between a molecule on the surface and the molecules below is the same for all of the molecules at the four sites, it is only necessary to consider differences in the effects of the neighboring surface molecules on the four molecules. Assuming *Y* is a strong interaction direction relative to *X,* to detach molecules 1 and 2, two strong interactions and one weak interaction with neighboring molecules need to be overcome; however, for molecules 3 and 4, only one strong interaction and two weak interactions need to be overcome. Therefore, it is easier to detach molecules at sites 3 and 4 than those at sites 1 and 2, that is, easier along the *Y* direction than the along the *X* direction.

In the dissolution process, incorporation of molecules is also affected by the directionally dependent attachment energy. Assuming that there is one surface diffusing molecule at the 0 lattice site and there are no molecules at sites 1, 2, 3, and 4, if the surface diffusion is only controlled by thermal motion, it will have the same probability to go to sites 1, 2, 3, and 4. Even though the free energy change during the incorporation process is different for sites 1 and 2 compared with sites 3 and 4, the probability of incorporation for one molecule should be the same for different sites. Because the probability is determined by the difference between the energy of the surface diffusing molecule and its transitional state and the transitional states can be assumed to be the same for joining different sites, the probabilities are the same. However, after incorporation, the probability of detachment is different. Therefore, the incorporation is actually controlled by the detachment process

(i.e., how often the diffusing molecule makes it to a site is controlled by probability, but how long it stays there is controlled by the energetics).

If the incorporation and detachment processes are repeated many times, the elongation pattern in the *Y* direction will be longer than that in the *X* direction and the relative length should depend on the relative strength of the attachment energies in each direction (in the simplest case). Overall, the model illustrated by Figure 8 shows that the etching patterns favor the direction with stronger attachment energies during the dissolution process via the incorporation and detachment processes of surface diffusion.

In the absence of specific interactions between solvent and crystal-bound molecules, the probability of detachment should be exponentially related to the relative energy (after Boltzmann). All of the involved attachment energies can be separated into two parts: projected energy on the face of interest and perpendicular energy related to the face. The perpendicular energy for molecules 1, 2, 3 and 4 on the same face should be the same. Therefore, only projected energies need to be taken into consideration when comparing the relative probability of detachment in different directions. Under given conditions of temperature and solvent with no molecule at the 0 site, the probability (*P*) of detachment can be expressed as

$$P_1 = P_2 = A' \exp\left(\frac{2E_y + E_x}{-B}\right) \tag{1}$$

$$P_3 = P_4 = A' \exp\left(\frac{2E_x + E_y}{-B}\right) \tag{2}$$

where E_x is the interaction between two neighboring molecules in the direction of *X* axis and E_y is the interaction in the direction of *Y* axis; A' and B are constants related to temperature and solvent solubilization ability. At constant temperature, solvents with higher solubilization ability will have a higher B value. Because $2(E_x + E_y)$ is the sum of all projected attachment energies on the face of interest, it can be treated as a constant for the specific face. The probability (*P*) of detachment in different directions can then be expressed as

$$P_i = A \exp\left(\frac{E_i}{B}\right) \tag{3}$$
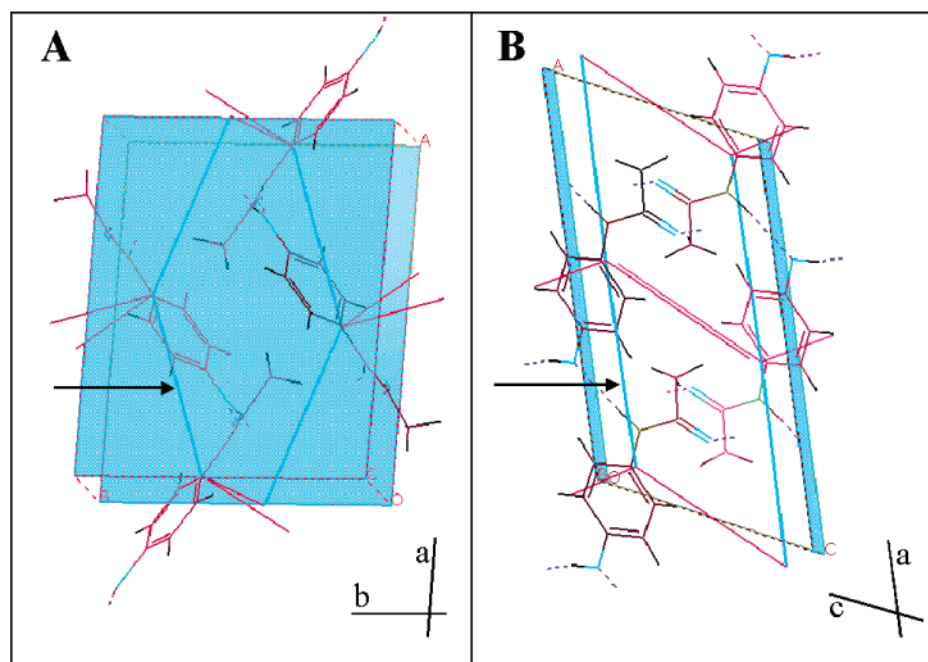
Figure 9. Periodic bond chains of acetaminophen calculated with Cerius[2]. The light blue faces (top in A and both edges in B) are the (001) face. The thick blue lines represent the strongest PBC force, and panel B shows that the thick blue lines are parallel to the (001) face and along the *a*-axis.

413 where E_i is the interaction between two neighboring molecules
414 in the direction of the *i*th axis; *A* and *B* are again constants
415 (determined by face, temperature, and solvent). Assuming that
416 the length of etching pit is linearly related to the probability of
417 detachment in different direction, then the ratio of length is

$$\frac{L_x}{L_y} = \frac{P_x}{P_y} = \exp\left(\frac{E_x - E_y}{B}\right) \qquad (4)$$

418 On the basis of eq 4, the etching patterns based on the projected
419 energies can be estimated when the effects of solvent-specific
420 interactions, temperature, etc. are ignored. Comparing the
421 predicted patterns with observed patterns may help to provide
422 more information about the interactions of solvent with crystal
423 surface during dissolution process.
424 **Comparison between Attachment Energies and Etching**
425 **Patterns on (001) and (110) Faces.** Each unit cell of the
426 acetaminophen crystal has four acetaminophen molecules, and
427 their geometrical centers of mass were used to determine the
428 directions of the PBC vectors (Figure 9). Because the lengths
429 of unit cell dimensions, *a*, *b*, and *c*, are not the same, the lengths
430 are basically expressed in fractional crystallographic coordinates
431 (i.e., the unit vectors **A**, **B**, and **C** are in the original directions
432 of the *a*-, *b*-, and *c*-axes, respectively, but with unit length one,
433 see Appendix). Table 4 shows the projections of nine dominant
434 PBC projections on the (001) face, as well as the complementary
435 perpendicular components (the calculations are explained in the
436 Appendix). Table 5 shows the projections of 16 dominant PBC
437 projections on the (110) face, as well as the complementary
438 perpendicular components. The PBCs of which the projections
439 are 10% or more of the maximum projection are listed in Tables
440 4 and 5, respectively. Table 6 shows the projection along the
441 directions of the *a*-, *b*-, and *c*-axes on different faces.
442 The main attachment energies may not always be parallel to
443 the faces of interest, and the contributions of those attachment
444 energies on the surface diffusion on the faces of interest may
445 be evaluated on the basis of their orthogonal projections on the
446 face. On the (010) face, the etching patterns show significant

TABLE 4: The Projections of Nine Dominant PBC Vectors onto the (001) Face and in the Direction Perpendicular to the (001) Face Sorted by Angles[a]

PBC	proj	A	B	perp	angle
		energy (kcal/mol)			
−3.73	−1.5231	−0.0678	0.9977	−3.4049	−86.16
−4.86	−4.6130	−0.0856	0.9963	−1.5296	−85.13
1.46	1.2847	0.4796	−0.8775	0.6937	−61.37
2.41	2.3298	0.8318	−0.5550	0.6167	−33.73
1.89	1.5512	0.8395	−0.5433	1.0797	−32.93
−11.64	−11.6400	0.9539	0.3003	0.0000	17.48
−4.95	−2.5944	0.8555	0.5178	−4.2156	31.20
−7.2	−5.3200	−0.8101	−0.5864	−4.8515	35.92
−7.59	−5.8634	−0.2123	−0.9772	−4.8196	77.78

[a] The **A** vector and **B** vector are the orthonormal bases of the (001) face and are used here to show the directions of the projected PBC vectors. PBC = attachment energy of the PBC vector; proj = projected energy on the (001) face; perp = projected energy along the direction perpendicular to the (001) face; angle = angle between the projection vector and the **A** vector.

447 elongation along both the *a*-axis and the *c*-axis. However, the
448 interaction values calculated by Li et al.[7] show that along the
449 *c*-axis, the attachment energies are not strong in the (010) face;
450 however, the attachment energies with upper and lower layers
451 are very strong. Even though the corresponding PBC vectors
452 of strong attachment energies are not parallel to the (010) face,
453 their effects are "projected" on the (010) face resulting in the
454 significant elongation along the *c*-axis.
455 For the (001) face, Table 4 clearly shows that the strongest
456 energy is in the **A** vector direction. This is coincident with the
457 direction of the *a*-axis projection on the (001) face. At
458 approximately 17°, the energy projection is −11.64 kcal/mol,
459 much larger than projections in any other direction, including
460 the combined projection energies of −86° and −85°. Of course,
461 some cumulative small projections also contribute to the strong
462 attachment energy in the direction of the *a*-axis. There also exists
463 one hydrogen-bond chain in the direction of the *a*-axis, and its
464 disruption may play a role in etching pattern formation. On the
465 basis of eq 4, if the energy difference in different directions is

H *J. Phys. Chem. B* Wen et al.

TABLE 5: The Projections of 16 Dominant PBC Projections on the (110) Face and in the Direction Perpendicular to the (110) Face[a]

energy (kcal/mol)					
energy	proj	**C**	**D**	perp	angle
−0.97	−0.8852	0.0328	−0.9995	−0.3967	−88.17
2.41	2.3971	−0.1219	0.9925	0.2489	−83.04
0.75	0.7334	0.2948	−0.9556	0.1570	−72.89
−11.64	−7.3881	0.6567	−0.7541	−8.9948	−48.97
−0.9	−0.8974	−0.6864	0.7272	−0.0682	−46.68
1.46	1.2711	−0.7027	0.7115	0.7182	−45.38
−7.59	−3.9458	0.9608	−0.2773	−6.4837	−16.11
0.82	0.7764	0.9984	−0.0573	0.2637	−3.29
−1.96	−1.9600	1.0000	0.0000	0.0000	0.00
−3.73	−3.1103	−0.9991	−0.0416	−2.0588	2.39
−7.2	−6.2754	−0.9955	−0.0949	−3.5299	5.45
−4.95	−3.5425	−0.7966	−0.6045	−3.4574	37.21
−1.24	−1.2152	−0.4230	−0.9061	−0.2467	65.01
−4.86	−3.8788	0.3102	0.9507	−2.9282	71.97
1.89	1.8528	0.2170	0.9762	0.3734	77.51
0.89	0.8904	0.0964	0.9953	0.0000	84.51

[a] The **C** vector and **D** vector (i.e, [0.865 −0.629 0.378]) are orthonormal bases of the (110) face and are used here to show the directions of the projected PBC vectors. PBC = attachment energy of the PBC vector; proj = projected energy on the (110) face; perp = projected energy along the direction perpendicular to the (110) face; angle = angle between projection vector and **C** vector.

TABLE 6: The Projection Directions of the *a*-, *b*-, and *c*-axes onto the Faces of Interest

face	(001)		(110)	
axis	[100]	[010]	[001]	[0.865 −0.629 0.378]
a	1	0	−0.53	0.85
b	0	1	0	−1
c	−1	0	1	0

466 large, the etching pattern will be dominated by the direction of
467 the strongest energy. Because the energy along the *a*-axis is
468 much stronger than that in other directions, the predicted etching
469 pattern will be needlelike in the direction of the *a*-axis. The
470 directions exhibiting weaker attachment energies such as along
471 the *b*-axis may also play a role in strong solvent, which is
472 consistent with the wider slit pattern by acetone than other
473 solvents. Overall, the etching pattern on the (001) face appears
474 to be under the guidance of the projections on the (001) face,
475 that is, the *a*-axis direction.

476 Table 5 shows that the attachment energies are not dominant
477 in any one direction for the (110) faces. There are several
478 directions with significant energy: in the direction of the *c*-axis
479 (from −16° to 5°), the energy is approximately −14 kcal/mol;
480 in the direction of −49°, approximately −7 kcal/mol; in the
481 direction of 70° (from 65°−77°), approximately −3 kcal/mol;
482 in the direction of 37°, about −3 kcal/mol. Based on eq 4, the
483 predicted etching patterns are shown in Figure 10 (for *B* values
484 of 3 and 10). As the solubilizing ability of solvent increases,
485 the effects of the minor projections become more important than
486 in weak solvent. All of the etching patterns have a dominant
487 feature along the *c*-axis, which is consistent with the dominant
488 projections along the *c*-axis. The predicted etching pattern with
489 *B* = 10 fits the observed etching patterns, which are arc-shaped,
490 for solvents including acetic anhydride, acetone, and pyridine,
491 as well as the water pattern. For dichloroethane, a weak solvent,
492 the observed etching pattern fits the predicted etching pattern
493 with *B* = 3. For ethyl acetate, the observed patterns look like
494 those predicted for a relatively weak solvent, even though ethyl
495 acetate has similar solubilizing ability as acetic anhydride. More
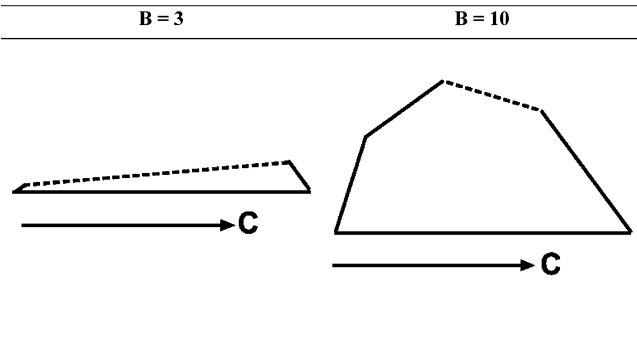496 study is needed to understand the difference of the predicted

Figure 10. Predicted etching patterns of acetaminophen (110) face under different *B* values.

497 and the observed etching patterns; however, this is clearly a
498 useful tool to probe the relative impact of solvent effects on
499 dissolution and crystallization. Overall, the PBC projections
500 combined with solubilizing ability approximately predict the
501 observed etching patterns on the (110) face (for most solvents).
502 This consistency supports the hypothesis that etching pattern is
503 affected by surface diffusion guided by the underlying crystal
504 interaction network.

505 The asymmetry of the etching patterns on the (110) faces
506 may be addressed by considering that both hydrogen-bond
507 chains cross the (110) face at an angle; on the other hand, Table
508 5 shows that most of the main PBC vectors cross the face at
509 yet a different angle. There is significant energy perpendicular
510 to the face. This asymmetry in the crystal structure and
511 attachment energies causes the asymmetry of the observed
512 etching patterns on the (110) faces.

513 For the (110) faces, the perpendicular energies are not
514 negligible compared to the projection energies, and it is not
515 clear what the effects are of those strong perpendicular energies
516 on surface diffusion. It is worthwhile to mention that for
517 acetaminophen crystallized in water, the unetched (110) face is
518 smooth and has no specific pattern but the unetched (001) face
519 exhibits a similar pattern as if it were etched by water. The
520 strong perpendicular energies may hinder the detachment of
521 molecules from the lattice on the (110) face; that is, the
522 difference of the perpendicular energies related to the two faces
523 may contribute to the difference in the unetched faces.

Summary 524

525 The predicted etching patterns based on the PBC projections
526 on the faces of interest and different *B* values (i.e., different
527 solubilizing ability of solvents) fit the observed etching patterns
528 well for most solvents on the (001) and (110) faces of
529 acetaminophen. The similarity further supports the idea that the
530 etching patterns are dictated by the internal crystal structure
531 through controlling surface diffusion of molecules based on the
532 attachment energies in different directions.

533 Etching patterns with prominent features in the direction of
534 the projection of the *c*-axis on the (110) face have been observed,
535 which is consistent with the etching patterns on the (010) face.
536 However, in the direction of the *a*-axis, the etching patterns are
537 highly solvent-dependent for the (110) and (010) faces. The
538 model shows that the projections contribute differently to etching
539 pattern formation depending upon the solvent. This may be the
540 main reason for the difference of the etching patterns differences
541 along the *a*-axis. As discussed, the existence of one hydrogen-
542 bond chain in the direction of the *a*-axis rather than in the
543 direction of the *c*-axis may also play a role in solvent adsorption
544 through hydrogen-bonding interactions and affect the etching
545 pattern formation.

Solvent adsorption onto a crystal surface can affect both the dissolution and crystallization processes. The most significant changes in etching patterns and crystal morphology are observed in dichloroethane, and the changes in both processes are consistent; that is, both changes suggest relatively strong adsorption in the direction of the *a*-axis or the *b*-axis or both. For other solvents, even though not as significant as the effects of dichloroethane, their effects cannot be ignored.

Overall, the etching patterns are mainly determined by the attachment energy in the face of interest, together with different solubilizing ability of solvents. With different solubilizing ability, solvent causes the surface diffusion time for acetaminophen on the crystal surface to vary. In weaker solvents, there is more time for surface diffusion, and the effects of weaker attachment energies become less important than in stronger solvents. In stronger solvents, the shorter surface diffusion time causes less difference in the contribution of weak and strong attachment energy on the etching pattern formation. After consideration of the effects of attachment energy and solubilizing ability of solvent, solvent adsorption effects may be better studied through observation of etching patterns and crystal morphology change compared to the predicted behavior.

Appendix

Originally, the PBC vector is in three-dimensional space, and the projection plane is in two-dimensional space. To project one PBC vector onto one specific plane, the transformation matrix needs to be calculated. Assuming the subspace W has an orthonormal basis $\{W1, W2\}$, then

$$\text{proj}_w(\mathbf{V}) = \sum_{i}^{2} \langle \mathbf{V}, W_i \rangle W_i$$

is the orthogonal projection of vector $\mathbf{V}$ onto the plane. Therefore, the projection matrix can be formed by using each orthonormal basis as a matrix column. Any vector $\mathbf{V}$ can be written uniquely as $\mathbf{V} = \mathbf{V}_w + \mathbf{V}_{w_\perp}$, here $V_w \in W$, $\mathbf{V}_{w_\perp} \in \mathbf{W}_\perp$, and $\mathbf{V}_w = \mathbf{V} - \mathbf{V}_{w_\perp}$.

The collected acetaminophen single crystals are monoclinic form with space group $P2_{1/a}$.[18] The cell constants are $a = 12.93$ Å, $b = 9.4$ Å, $c = 7.1$ Å, $\alpha = \gamma = 90°$, and $\beta = 115.9°$. Let $\mathbf{A}, \mathbf{B}$, and $\mathbf{C}$ represent the unit vectors along the *a*-, *b*- and *c*-axes respectively, and all vectors can be represented in terms of $\mathbf{A}$, $\mathbf{B}$, and $\mathbf{C}$. The three axes of one unit cell can be represented as

$$a = 12.93\mathbf{A}, \quad b = 9.4\mathbf{B}, \quad c = 7.1\mathbf{C}$$

The dot products between two unit vectors are

$$\mathbf{A} \cdot \mathbf{A} = \mathbf{B} \cdot \mathbf{B} = \mathbf{C} \cdot \mathbf{C} = 1, \quad \mathbf{A} \cdot \mathbf{B} = \mathbf{C} \cdot \mathbf{B} = 0,$$
$$\mathbf{A} \cdot \mathbf{C} = 1 \times 1 \times \cos \beta = -0.437$$

$$\mathbf{V}_{\text{unit}} = \frac{\mathbf{V}}{|\mathbf{V}|} = \frac{\mathbf{V}}{\sqrt[2]{u^2 + v^2 + w^2 + 2uw \cos \beta}}$$

Vector $\mathbf{V} = u\mathbf{A} + v\mathbf{B} + w\mathbf{C}$ can be represented as $[uvw]$ and its unit vector.

Note that the vector here is not the same as the vector represented in terms of crystal unit cell. That means a crystal vector $\mathbf{V} = ua + vb + wc = 12.93u\mathbf{A} + 9.4v\mathbf{B} + 7.1w\mathbf{C}$. For two vectors $\mathbf{V}_1 = [u_1v_1w_1]$ and $\mathbf{V}_2 = [u_2v_2w_2]$, the dot product is

$$\mathbf{V}_1 \cdot \mathbf{V}_2 = u_1u_2 + v_1v_2 + w_1w_2 + u_1w_2 \cos \beta + u_2w_1 \cos \beta$$

For each PBC vector, from the two molecule positions, its direction can be represented using unit vectors. The PBC bond energy can be used as the length of the PBC vector. For the (001) face of acetaminophen crystals, it is easy to see that the plane has two orthonormal bases, [100] and [010], which are perpendicular to each other. For (110) face of acetaminophen crystals, the plane has two orthonormal bases [001] and [0.865 − 0.629 0.378]. Then the orthogonal projection matrixes are

$$\mathbf{M}(001) = \begin{bmatrix} 1 & 0 & 0 \\ 0 & 1 & 0 \\ 0 & 0 & 0 \end{bmatrix} \qquad \mathbf{M}(110) = \begin{bmatrix} 0 & 0.865 & 0 \\ 0 & -0.629 & 0 \\ 1 & 0.378 & 0 \end{bmatrix}$$

References and Notes

(1) Chan, H. K.; Grant, D. J. W. *Int. J. Pharm.* **1989**, *57*, 117.
(2) Dali, M. V.; Carstensen, J. T. *Pharm. Res.* **1996**, *13*, 155.
(3) Danesh, A.; Connell, S. D.; Davies, M. C.; Roberts, C. J.; Tendler, S. J. B.; Williams, P. M.; Wilkins, M. J. *Pharm. Res.* **2001**, *18*, 299.
(4) Burt, H. M.; Mitchell, A. G. *Int. J. Pharm.* **1981**, *9*, 137.
(5) Burt, H. M.; Mitchell, A. G. *Int. J. Pharm.* **1979**, *3*, 261.
(6) Radenovic, N.; van Enckevort, W. *J. Cryst. Growth* **2002**, *234*, 589.
(7) Li, T.; Morris, K. R.; Park, K. *J. Phys. Chem. B* **2000**, *104*, 2019.
(8) Vasil'chenko, M. A.; Shakhtshneider, T. P.; Naumov, D. Y.; Boldyrev, V. V. *J. Pharm. Sci.* **1996**, *85*, 929.
(9) Plomp, M.; van Enckevort, W. J. P.; Vlieg, E. *J. Cryst. Growth* **2000**, *216*, 413.
(10) Sakaino, K.; Adachi, S. *Sens. Actuators, A* **2001**, *A88*, 71.
(11) Khoshkhoo, S.; Anwar, J. *J. Phys. D: Appl. Phys.* **1993**, *26*, B90.
(12) Hartman, P.; Perdok, W. G. *Acta Crystallogr.* **1955**, *8*, 49.
(13) Hartman, P.; Perdok, W. G. *Acta Crystallogr.* **1955**, *8*, 521.
(14) Hartman, P.; Perdok, W. G. *Acta Crystallogr.* **1955**, *8*, 525.
(15) Wittmuess, D.; Kueppers, H. The morphology of potassium trihydrogen dioxalate dihydrate, KH₃(C₂O₄)2.2H₂O. *Z. Kristallogr.* **1994**, *209*, 232.
(16) Nadarajah, A.; Pusey, M. L. *Acta Crystallogr.* **1996**, *D52*, 983.
(17) Weissbuch, I.; Shimon, L. J. W.; Landau, E. M.; Popovitz-Biro, R.; Berkovitch-Yellin, Z.; Addadi, L.; Lahav, M.; Leiserowitz, L. *Pure Appl. Chem.* **1986**, *58*, 947.
(18) Haisa, M.; Kashino, S.; Kawai, R.; Maeda, H. *Acta Crystallogr.* **1976**, *B32*, 1283.
(19) Jones, E. C.; MacPherson, J. V.; Unwin, P. R. *J. Phys. Chem. B* **2000**, *104*, 2351.
(20) Kuznetsov, Y. G.; Konnert, J.; Malkin, A. J.; McPherson, A. *Surf. Sci.* **1999**, *440*, 69.
(21) Yip, C. M.; Ward, M. D. *Biophys. J.* **1996**, *71*, 1071.
(22) Malkin, A. J.; Kuznetsov, Y. G.; Lucas, R. W.; McPherson, A. *J. Struct. Biol.* **1999**, *127*, 35.
(23) Kitamura, M.; Onuma, K. *J. Colloid Interface Sci.* **2000**, *224*, 311.
(24) Mauri, A.; Moret, M. *J. Cryst. Growth* **2000**, *208*, 599.
(25) Shindo, H.; Ohashi, M. *Appl. Phys. A: Mater. Sci. Process.* **1998**, *66*, S487.
(26) Boerrigter, S. X. M.; Cuppen, H. M.; Ristic, R. I.; Sherwood, J. N.; Bennema, P.; Meekes, H. *Cryst. Growth Des.* **2002**, *2*, 357.
(27) Cang, H.-X.; Huang, W.-D.; Zhou, Y.-H. *J. Cryst. Growth* **1998**, *192*, 236.
(28) ter Horst, J. H.; Geertman, R. M.; van Rosmalen, G. M. *J. Cryst. Growth* **2001**, *230*, 277.
(29) Ristic, R. I.; Finnie, S.; Sheen, D. B.; Sherwood, J. N. *J. Phys. Chem. B* **2001**, *105*, 9057.
(30) Chow, A. H. L.; Grant, D. J. W. *Int. J. Pharm.* **1988**, *42*, 123.